Draft Technical Summary Report

Results from I76 Viaduct Vibration Survey

Submitted to:

PennDOT District No. 6

Prepared by:

John Braley and Frank Moon
Rutgers University

Charles Young, Ivan Bartoli and Emin Aktan
Drexel University

August 2016

Introduction

Test Structure Description

Photo of bridge elevation

Description

The viaduct was first constructed in 1952. The superstructure was replaced in 1986, while reusing the original piers and foundations. The structure runs along the banks of the Schuylkill River and carries the Schuylkill Expressway (I-76) with a total of four lanes of traffic. Bridge users have reported experiencing unusually high levels of vibration while on the structure.

Network

The bridge is located between mile 338 and 339 of Interstate 76 (Schuylkill Expressway) and carries more than 57,000 vehicles a day with 4% truck traffic. The bridge spans an access road and a railroad (spans 9 & 10). Testing of this bridge will not require access in the vicinity of the railroad.

Superstructure

The structural type is steel multi-girder. Eight girders run longitudinally, resting on steel box girders that span transversely and are supported by the concrete piers. A reinforced concrete composite deck was cast in place, with a “raked” finish and no overlay. There is no skew. The bridge has eleven spans. The maximum span length is 140’-0”. The out-to-out width is 76’-6”. Three spans are simply supported, while the remaining eight are two-span continuous. Each span has five interior rows of X-framed diaphragms and chevron diaphragms over the piers.

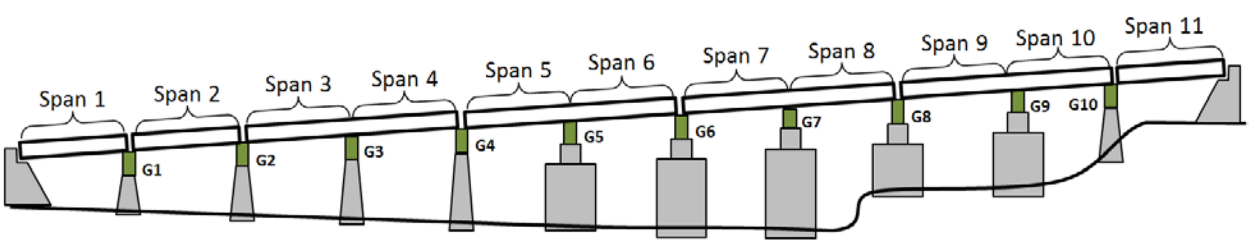

Diagram of Bridge System

Substructure and Bearings

The concrete piers and abutments were constructed in 1952 and are all that remains of the original structure. They are supported by driven piles. Elastomeric bearing pads are installed on top of the piers and support the transverse box girders. Rocker bearings or pedestals are installed between the box girders and longitudinal girders at those locations which are in the center of continuous spans. Elastomeric bearings are installed between the box girder and the longitudinal girders at the remaining locations.

Bearings under Continuous Spans

Condition

Visually, the deck appears to be in good condition, with no major cracking visible. Minor damage was observed in some regions of the center concrete barrier. The girders appeared in excellent condition. No major rusting was observed, and the girders appeared well maintained. The access hatches on many of the box girders had been left open. Any ill effects from this could not be immediately observed. The piers exhibited very little efflorescence and virtually no spalling. Repairs had been performed on several piers, where an embedded drainage pipe had rusted and caused a portion of concrete to spall off.

NBI Details

NBI Structure Number	**000000000027280**
Year Reconstructed	1986
Owner	PennDOT
Skew	0 degrees
Deck Width	76’-6”
Maximum Span Length	140’-0”
ADT	57410 (2013)
Deck Condition	6 (Satisfactory Condition)
Superstructure Condition	7 (Good Condition)
Substructure Condition	5 (Fair Condition)
Sufficiency Rating	70

Test Objectives

Members of this group were notified by PennDOT officials that concerned bridge users had been reporting high vibration levels. It was the purpose of this testing effort to identify the nature of the vibrations and their magnitude. It is of secondary concern to identify if the levels of vibration are detrimental to the structure, and recommend methods of reducing the vibration if such is the case.

Testing Activities

Preliminary Survey of Cross Girder Acceleration

Preliminary testing of the viaduct took place on July 6th and 7th. The cross girders at piers 2, 3, 5 and 7 were instrumented with accelerometers.

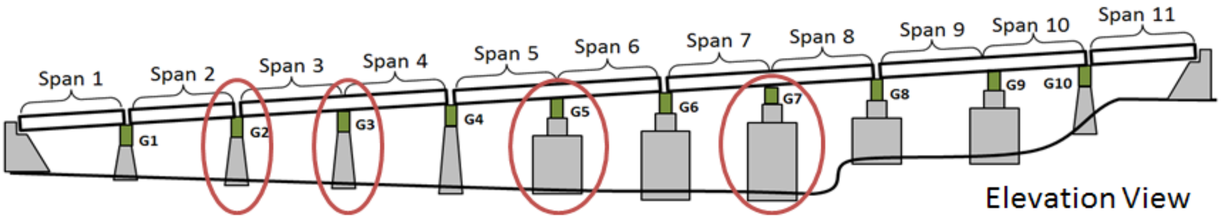

Locations of Instrumented Cross Girders

The acceleration of these members due to traffic was recorded in an effort to determine the spans with the highest levels of vibration. The cross girders all experienced similar levels of vertical and longitudinal acceleration, while the cross girder at pier 7 experienced much higher transverse acceleration.

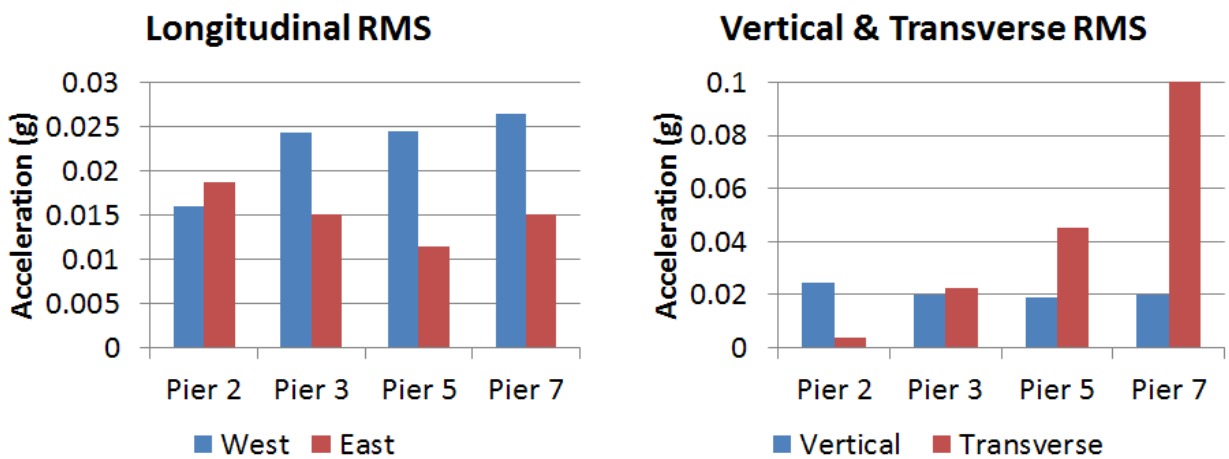

Plot of Root Mean Square of Acceleration during Preliminary Survey

As a result, spans 7 and 8 were chosen for the in depth investigation.

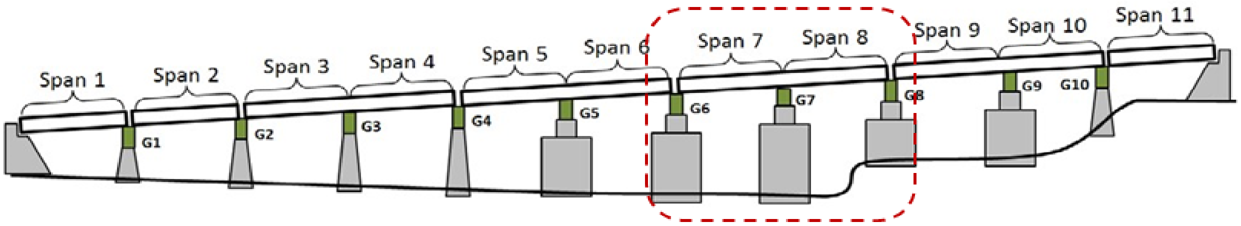

Chosen Spans for Full Investigation

In Depth Vibration investigation

Instrumentation of spans 7 and 8 was performed on July 26th and 27th. Data was recorded on July 27th and 28th. Sensors were removed on July 29th.

Accelerometer **Strain Gauge**

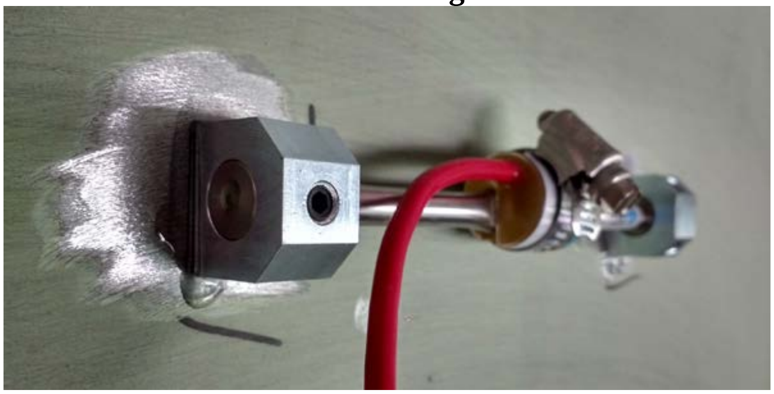

Sensor Types Used in Test

A total of 30 accelerometers (PCB Model 393A03) and 12 strain gauges (Geokon 6" vibrating wire) were installed on the chosen region of the viaduct. Epoxy was used to attach the strain gauges to the steel surface (after paint was removed).

They were located (as depicted in the images below) so as to capture maximum response as well as to characterize the mode (shape) of vibration.

Accelerometer Instrumentation

Accelerometers were installed to the steel superstructure via magnets that were attached to the accelerometer base. Accelerometers were installed on the pier with hot-glue. Cables were run along the girders to Pier 7, and down to the ground at Pier 7. The accelerometers were sampled with National Instruments CompactRIO with 8 NI 9234 cards installed and using a LabVIEW acquisition program. The acquisition system sampled at 200 Hz for multiple hours at a time over a period of 2 days, recording a total of 14 hours of data.

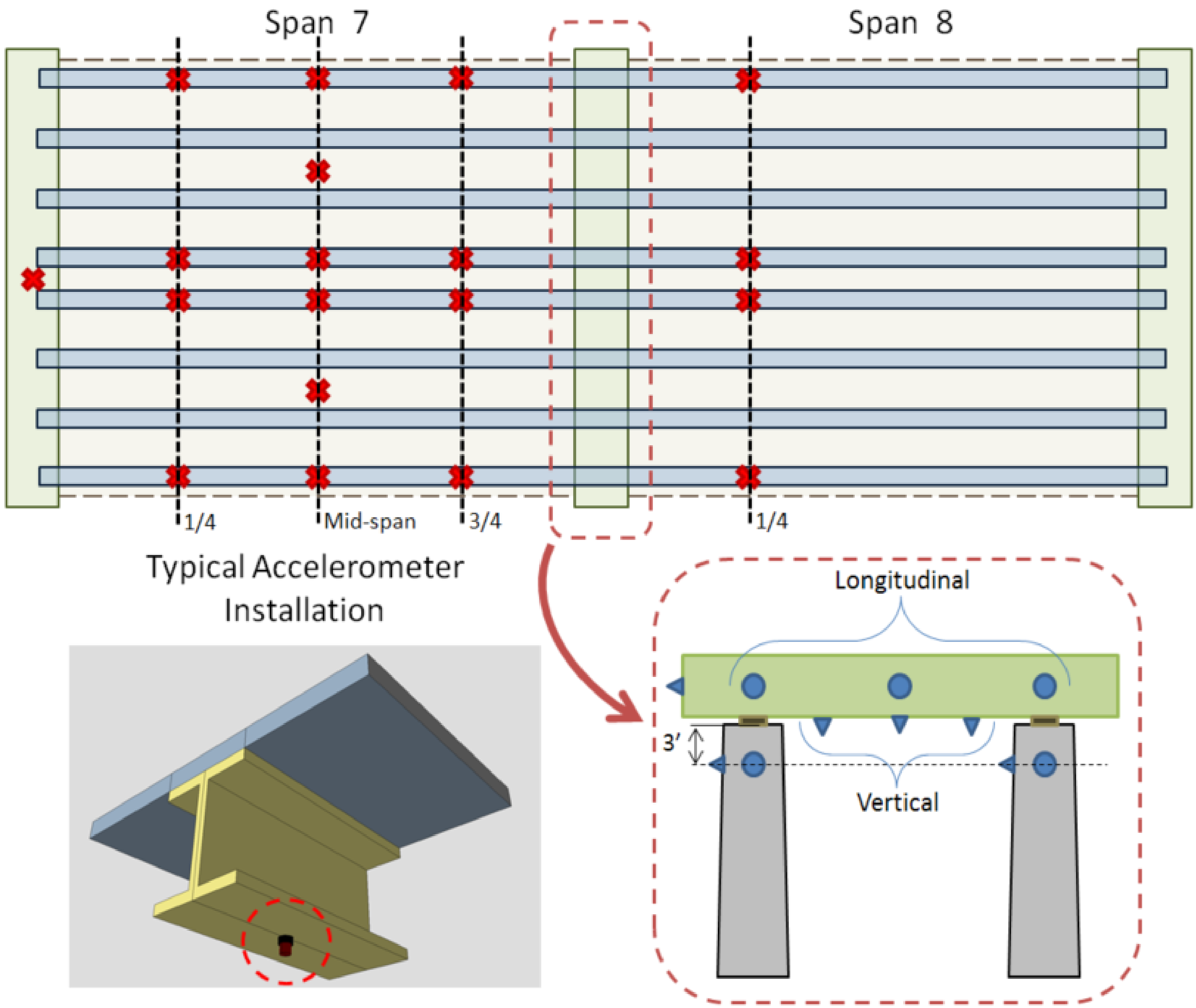

Layout and Details of Accelerometer Installation

Strain Gauge Layout

The locations where strain gauges were to be installed were identified and the paint removed with an angle grinder equipped with sandpaper disks until bare metal was exposed. This surface treatment is essential for proper adhesion of the gauge. Epoxy was applied to the strain gauge bases before being positioned on the treated surface. Duct tape was used to temporarily hold the gauge in place while the epoxy cured. After at least 8 hours of curing the duct tape was removed, the gauge set screws were loosened and then retightened to release any intrinsic forces. The cables were run along the girders toward Pier 7 and to the ground at Pier 7. The strain gauges were sampled using a Campbell Scientific CR6 Datalogger with 2 CDM-VW305 8 Channel Vibrating Wire Analyzers. The system sampled at 50 Hz for 12 hours, and at 20 Hz for 8 hours during the night.

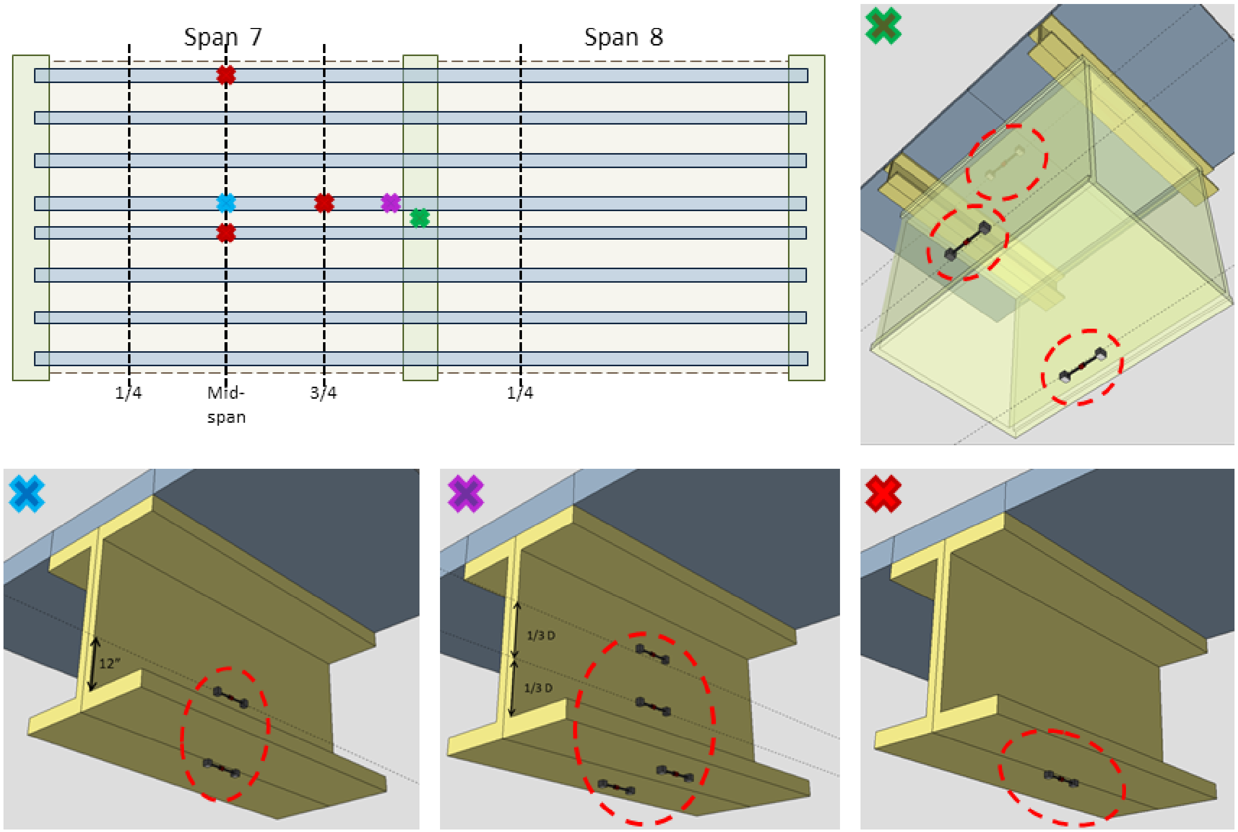

Layout and Details of Strain Gauge Installation

Acceleration Results

Time History

The a low-pass filter was applied to the acceleration data in an effort to remove high frequency acceleration (above 20 Hz) from sources such as noise and member local modes that could cloud global vibration characteristics. The root mean square was calculated for every 20 minute period of the data to track the change in the level of excitation over time.

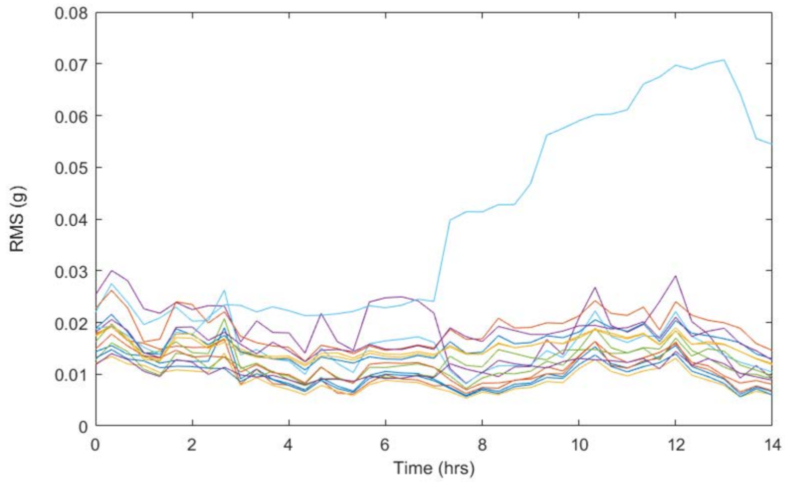

RMS of Superstructure DOF over Time

As can be seen from the above plot, the superstructure experiences relatively steady vibration and it increases toward the latter half of the total record. This time corresponds to the period between 12:00 PM and 3:30 PM. The maximum RMS values for the superstructure range from 0.015 to 0.07 g. In contrast, the RMS values for the pier accelerometers did not exceed 0.003 g. This is due to the effectiveness of the bearings, isolating the pier from superstructure vibrations, and the comparatively large axial stiffness of the piers which limits (and effectively prevents) vertical pier acceleration: the direction for which the superstructure experiences the greatest vibration.

Vibration Characterization

The acceleration data was analyzed using Fourier transform methods to extract information about the acceleration at specific frequencies.

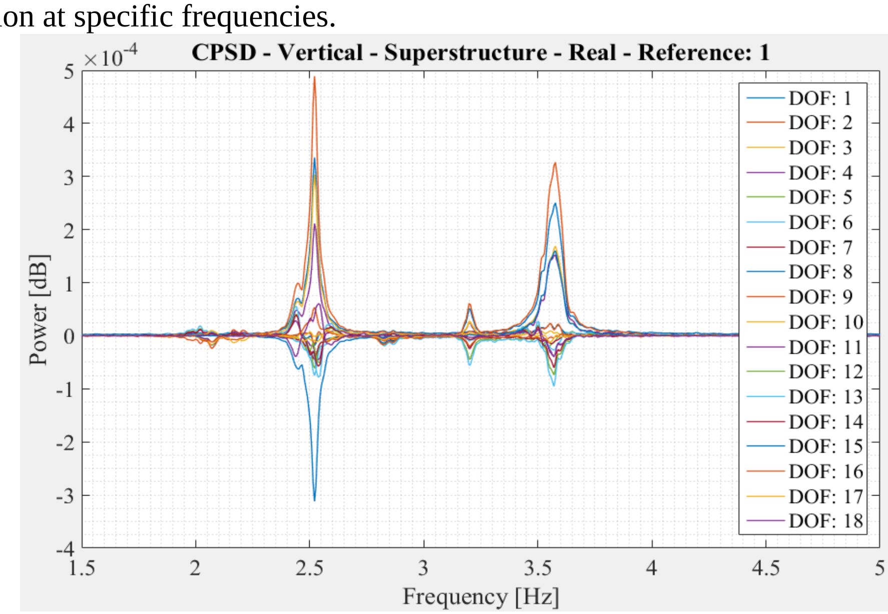

Cross Power Spectral Density of Superstructure DOFs

Several modes of vibration were found at frequencies below 5 Hz. The image above shows the power of each frequency. The peaks in the plots are poles where a mode of vibration is occurring, and for this structure, a natural frequency. In some instances, poles are at very similar frequency and the separate peaks cannot be easily distinguished. This is due to the geometry of the structure (high degree of symmetry) and the fact that there are essentially two identical bridges adjacent to one another. The main modes identified by this effort consisted of bending and torsional modes. For these modes, the mid-span degrees of freedom are experiencing the greatest acceleration. The shapes of several of these modes are displayed below.

Mode with One Side Active	Mode with Spans Out of Phase	Mode with Spans in Phase
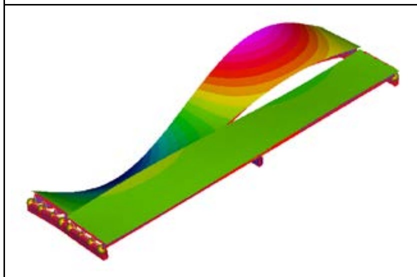	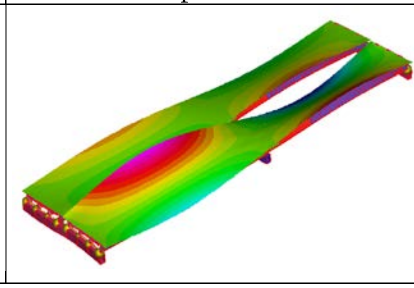	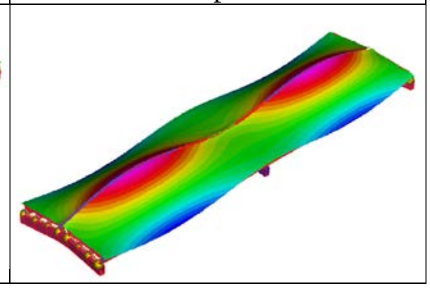

Common Types of Vibration Shapes (Mode Shapes)

Strain Results

Operational Strain and Stress

A total of 12 strain gauges were installed and data recorded for more than 24 hours. Gauges were sampled at 50 Hz which allowed us to capture the dynamic behavior of the bridge.

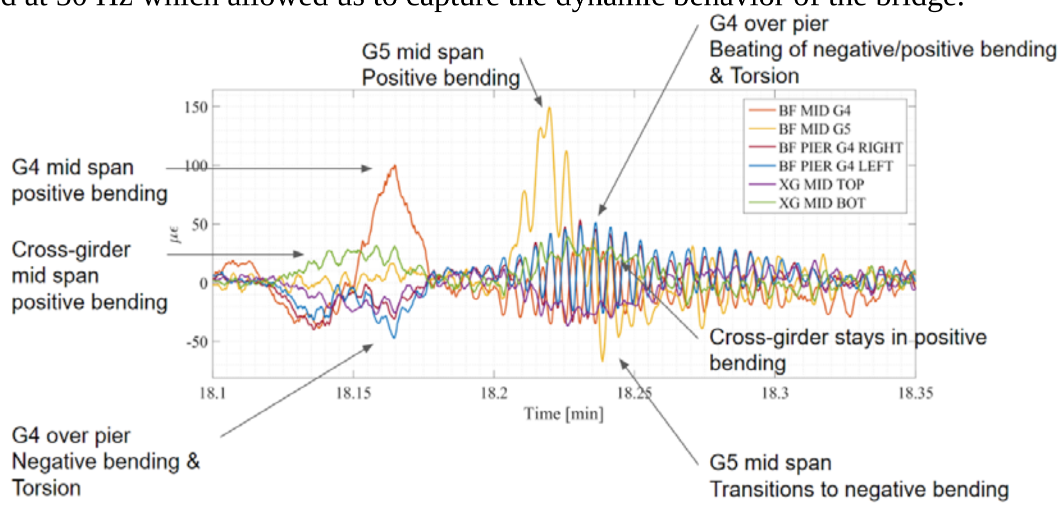

Strain Response

Strain levels in excess of 100 microstrain (3 ksi) were not uncommon, and occasional responses as high as 6 ksi were recorded in the bottom flange of longitudinal girders at mid-span. The interior girders (supported at the center of the box girder) experienced the highest responses. A low pass filter was applied to the data to remove the data associated with frequencies above 1.5

Hz, thus permitting the dynamic response of the bridge to be removed from the data and only the static response of the bridge to be plotted.

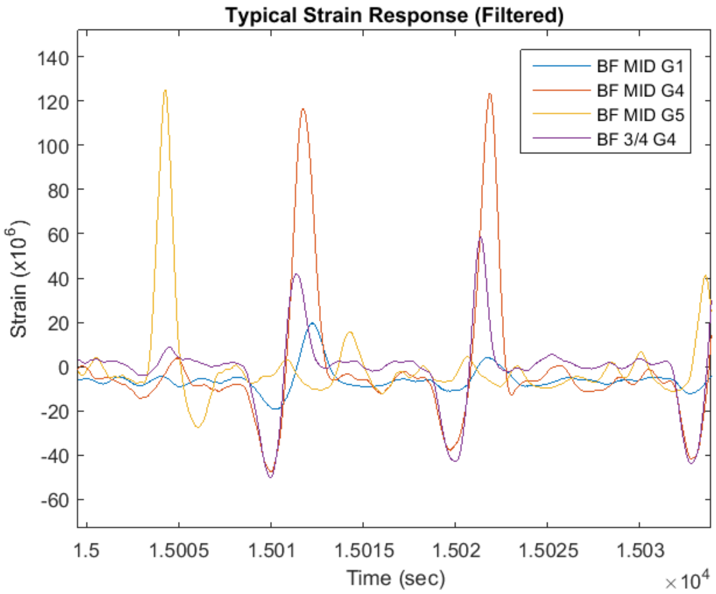

Typical Static Strain Response Under Operational Traffic Loading

Dynamic Amplification

The strain data plotted above has been filtered to show only the static response. The additional strain due to the vibration of the bridge is neglected. However, the portion of strain due to the dynamic response (vibration) of this structure is significant. The plot below is during a large event. The static response accounts for over 100 microstrain, but the vibration of the structure causes the total response to exceed 200 microstrain. For this event, an amplification of the static response by approximately 75% is observed. In comparison, the amplification applied for bridge design is only 33% or less.

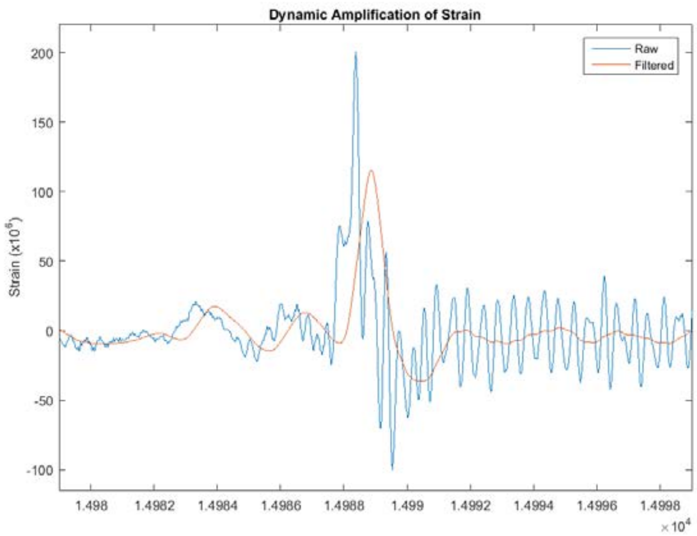

Dynamic Amplification of Strain

This level of amplification is on the upper end of what researchers and transportation organizations have measured. However, the fact that the high amplification occurs regularly and even with large events, makes the nature of this bridge's response quite novel.

Calculated Fatigue Life

As the magnitude and frequency of strain responses were quite high, a fatigue life analysis was performed to investigate whether the components at the sensor locations were in danger of fatigue failure. A Rain Flow analysis with subsequent application of Miner's Rule was performed on the strain data collected to obtain estimates of fatigue life based on the cycles of strain measured. These fatigue life estimates are not for the entire structure, but only for those components that were instrumented and at the location of the installed gauge. Furthermore, the fatigue lives were based on the operational response of the structure during the two days of testing. This level of response, while expected to be representative of the typical response, is not guaranteed to be constant throughout the life of the bridge. Therefore, the quantities presented below serve to demonstrate the level of the structure's resistance to fatigue. They do not predict the time until fatigue failure.

Fatigue Life (years)

Fatigue Category	BF MID G1	BF MID G4	BF MID G5	BF 3/4 G4	RIGHT BF	LEFT BF	XG MID BOT
A	25042	9290.6	6513.8	49420	34513	32594	115360
B	12020	4459.5	3126.6	23722	16566	15645	55372
C	4407.4	1635.1	1146.4	8697.9	6074.2	5736.6	20303

These results suggest that in spite of high operational stress, these components are not vulnerable to fatigue.

Conclusions and Future Work

Preliminary analysis of acceleration and strain data has provided the magnitude and nature of vibration being experienced by the structure. The magnitudes measured are significantly larger than what is usually measured under operational loading.

The cause for this elevated response has not yet been determined. There are many mechanisms that may be responsible for or contribute to the phenomenon, including unique bridge geometry, specific traffic patterns, or dynamic amplification with unusual vehicle/bridge interaction.

Investigation to identify and understand the mechanism or mechanisms at play will continue over the coming months. If action is deemed advisable, recommendation will be delivered.